Journal of Fluorescence, Vol. 16, No. 2, March 2006 (© 2006)
DOI: 10.1007/s10895-005-0036-x

Non-Uniform Membrane Probe Distribution in Resonance Energy Transfer: Application to Protein–Lipid Selectivity

Ricardo C. Capeta,[1] José A. Poveda,[2] and Luís M. S. Loura [1,3,4]

Received September 14, 2005; accepted November 11, 2005
Published online: March 11, 2006

Biological membranes are, at the molecular level, quasi-two dimensional systems. Membrane components are often distributed non-uniformly in the bilayer plane, as a consequence of lipid phase separation/domain formation or local enrichment/depletion of particular lipid species arising form favorable/unfavorable lipid–membrane protein interactions. Due to its explicit dependence on donor–acceptor distance or local acceptor concentration, resonance energy transfer (RET) has large potential in the characterization of membrane heterogeneity. RET formalisms for the basic geometric arrangements relevant for membranes have now been known for several decades. However, these formalisms usually assume uniform distributions, and more general models are required for the study of membrane lateral heterogeneity.

We present a model that addresses the possibility of non-uniform acceptor (e.g., lipid probe) distribution around each donor (e.g., protein) in a membrane. It considers three regions with distinct local acceptor concentration, namely, an exclusion zone, the membrane bulk, and, lying in between, a region of enhanced probability of finding acceptors (annular region). Numerical solutions are presented, and convenient empirical fitting functions are given for RET efficiency as a function of bulk acceptor surface concentration, for several values of the model parameters. The usefulness of the formalism is illustrated in the analysis of experimental data.

KEY WORDS: Fluorescence; FRET; lipid bilayer; membrane protein; lipid–protein interaction.

INTRODUCTION

The original formulation of resonance energy transfer (RET), as carried out by Förster, assumed uniform distribution of donors and acceptors in an infinite medium [1]. However, this is not necessarily the case in several systems, such as crystals [2], polymers, [3] or biological membrane models. Specifically for the latter, nonuniform probe distribution may result from probe aggregation, lipid phase separation, or differential lipid affinity for the immediate vicinity of a membrane protein, the so-called annular region (see Ref. [4] for a review of RET in nonhomogeneous membrane systems). In these systems, RET data analysis with adequate models may lead to recovery of relevant biophysical information, such as probe partition coefficients, phase boundary limits and estimation of domain sizes in lipid mixtures [5, 6], or lipid selectivity constants for a given membrane protein.

Regarding the latter, to our knowledge, two models have been used in past studies. The first one is based on approximate analytical expressions for the average rate of RET ($\langle k_T \rangle$) in membranes undergoing phase separation or protein aggregation, derived by Gutierrez-Merino [7, 8]. This author later extended his formalism to the study of protein–lipid selectivity [9–11]. This simple model has some limitations, namely, the simplification that underlies

[1] Centro de Química e Departamento de Química, Universidade de Évora, Évora, Portugal.
[2] Instituto de Biología Molecular y Celular, Universidad Miguel Hernández, Elche, Spain.
[3] Centro de Química-Física Molecular, Instituto Superior Técnico, Lisboa, Portugal.
[4] To whom correspondence should be addressed. E-mail: pclloura@alfa.ist.utl.pt

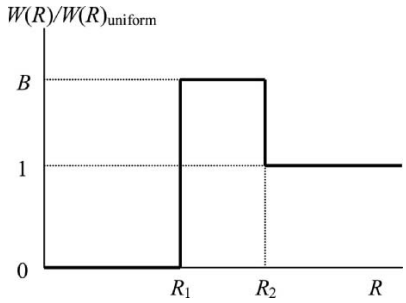

Fig. 1. Plot of the ratio between the acceptor distribution function considered in the present model and that for uniform distribution (e.g., $2R/R_d^2$ for a planar disk), showing the parameters R_1, R_2, and B.

the formalism, which consists of considering RET only to neighboring acceptor molecules. On the other hand, the experimental observable being the average RET efficiency given by

$$\langle E \rangle = \left\langle \frac{k_T}{k_T + k_D} \right\rangle \quad (1)$$

where k_D is the donor intrinsic decay rate coefficient, the relationship to $\langle k_T \rangle$ is not straightforward. It is proposed that if the setting of experimental conditions is such that $\langle E \rangle$ is low (namely, $\langle k_T \rangle$ is much smaller than k_D), then $\langle E \rangle \cong \langle k_T \rangle / k_D$ [7]. However, low accurate RET efficiencies are difficult to measure experimentally.

A second formalism was recently used by Fernandes *et al*. in the characterization of the lipid selectivity by the M13 bacteriophage major coat protein [12]. This protein has a single transmembrane segment, around which an annular region consisting of a single phospholipid layer (12 lipid molecules) was considered. Naturally, the application of this formalism to larger proteins, for which the number of lipid molecules in the annular region is unknown, is not immediate. On the other hand, the somewhat complex equations of this formalism limit its appeal for potential users.

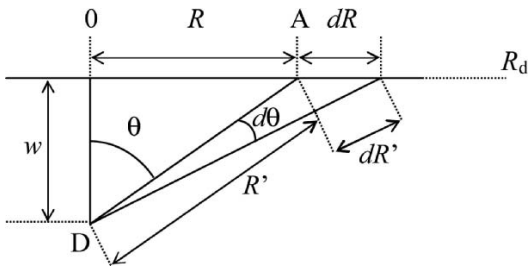

Fig. 2. Spatial geometry for RET in bilayer geometry (between donors in a plane and acceptors in another, parallel to that of donors; adapted from Ref. [16]).

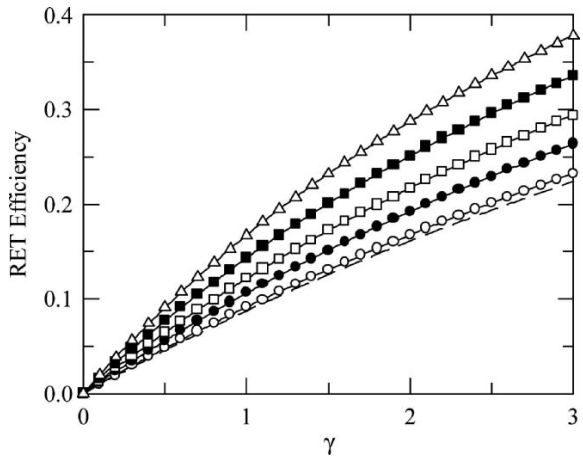

Fig. 3. RET efficiency as a function of dimensionless acceptor concentration $\gamma = n\pi R_0^2$ for planar geometry ($\beta_w = w/R_0 = 0$) and $\beta_1 = R_1/R_0 = 1.50$. Numerical results (○: $B = 1.05$; ●: $B = 1.25$; □: $B = 1.50$; ■: $B = 2.00$; △: $B = 3.00$) and empirical fits (*solid lines*) are shown for different values of the factor of acceptor annular enrichment, B. The previously obtained result (numerical integration of the decay law given in Ref. [13]) for $B = 1.00$ (uniform distribution outside the exclusion region) is also shown for comparison (*dashed line*).

In this report, an alternative formalism for RET in membranes with lipid–protein selectivity is proposed. It is inspired in the distribution function used by Rotman and Hartmann in three-dimensional crystals [2], in that, around each donor, three regions are considered: (i) an exclusion region closest to the donor ($R < R_1$), reflecting the radius of the protein; (ii) the annular region ($R_1 < R < R_2$), for which there is an increased probability of finding acceptors, characterized by a parameter B; and (iii) a region for which the acceptor concentration is equal to the overall value ($R > R_2$). The resulting local acceptor concentration is a step-function of the donor–acceptor distance, as shown in Fig. 1. The actual derivation of the donor decay law is considerably different to that presented by Rotman and Hartmann for three-dimensional media, because, in addition to planar geometry (for which adaptation of these authors' model would be straightforward), we consider the more general situation of donors and acceptors located in distinct parallel planes in the bilayer. In addition, and taking into account the complexity of the final equations, we present fitting parameters of empirical equations to the numerical exact RET efficiency results (similarly to previous RET theoretical studies for different topologies [13, 14]), which can be easily used by experimental researchers who wish to obtain a rapid estimate of the relative enrichment of a given component in the annular region. Finally, we illustrate this method with the analysis of published RET data between the tryptophan

Table I. Best Fit Parameters A_i of Eq. (22) to the Numerical Results Obtained for $\beta_w = 0$

	β_1							
	0.20	0.40	0.60	0.80	1.00	1.25	1.50	2.00
				$B = 1.05$				
A_0	0.33160	0.36971	0.45075	0.57177	0.70518	0.83413	0.90841	0.96820
A_1	−0.76090	−0.75470	−0.72460	−0.63981	−0.50310	−0.32270	−0.19200	−0.07020
A_2	0.12356	0.06215	−0.04910	−0.17210	−0.25010	−0.24210	−0.17780	−0.07700
A_3	0.52348	0.49434	0.42057	0.27734	0.10443	−0.03980	−0.07850	−0.05130
A_4	0.19398	0.20390	0.20916	0.17691	0.10819	0.02619	−0.01130	−0.01630
				$B = 1.25$				
A_0	0.32930	0.33966	0.40475	0.52656	0.66806	0.80959	0.89357	0.96270
A_1	−0.76270	−0.75330	−0.72560	−0.66008	−0.53920	−0.36010	−0.21970	−0.08210
A_2	0.12603	0.11722	0.03039	−0.11279	−0.22580	−0.24970	−0.19490	−0.08860
A_3	0.52707	0.51155	0.44731	0.32318	0.15186	−0.01560	−0.07500	−0.05710
A_4	0.19517	0.18937	0.18918	0.17830	0.12580	0.04173	−0.00530	−0.01740
				$B = 1.50$				
A_0	0.32926	0.33304	0.37594	0.48840	0.63318	0.78501	0.87821	0.95686
A_1	−0.76280	−0.75770	−0.72820	−0.67211	−0.56800	−0.39490	−0.24730	−0.09450
A_2	0.12600	0.12536	0.07881	−0.05901	−0.19680	−0.25210	−0.20960	−0.10030
A_3	0.52711	0.52154	0.46671	0.35464	0.19329	0.01121	−0.06840	−0.06240
A_4	0.19520	0.19212	0.17899	0.17301	0.13771	0.05721	0.00195	−0.01820
				$B = 2.00$				
A_0	0.32926	0.33076	0.35569	0.44797	0.58987	0.75161	0.85638	0.94827
A_1	−0.76280	−0.76040	−0.73560	−0.68323	−0.59780	−0.43800	−0.28470	−0.11250
A_2	0.12600	0.12653	0.10871	$-8.36E-04$	−0.15450	−0.24810	−0.22600	−0.11650
A_3	0.52711	0.52533	0.48841	0.38552	0.23991	0.04996	−0.05470	−0.06860
A_4	0.19520	0.19399	0.17905	0.16522	0.14671	0.07713	0.01375	−0.01860
				$B = 3.00$				
A_0	0.32926	0.33001	0.34562	0.41761	0.54983	0.71687	0.83230	0.93835
A_1	−0.76280	−0.76150	−0.74270	−0.69353	−0.62110	−0.47820	−0.32360	−0.13290
A_2	0.12600	0.12647	0.12017	0.04167	−0.11100	−0.23650	−0.23850	−0.13370
A_3	0.52711	0.52639	0.50287	0.41170	0.27911	0.09126	−0.03500	−0.07370
A_4	0.19520	0.19464	0.18305	0.16183	0.15061	0.09571	0.02797	−0.01800

residues of the nicotinic acetylcholine receptor (AcChR) from *Torpedo marmorata* to *trans*-parinaric acid (*t*-PnA) in egg phosphatidylcholine (egg-PC)/1,2-dimirystoyl-*sn*-glycero-phosphatidic acid (DMPA)/cholesterol (2:1:1) vesicles [15].

THEORY

The starting point is the usual set of approximations for derivation of the RET kinetics for an ensemble of acceptors, that is:

1. Donors and acceptors interact through the dipolar mechanism, in the very weak coupling limit;
2. The number of excited donors is negligible relative to the number of acceptor molecules;
3. Homotransfer among donors is neglected;
4. Translational diffusion during the donor excited state lifetime is neglected;
5. There is a single Förster distance R_0 for all donor–acceptor pairs.

Let us focus on one donor molecule. The overall rate coefficient of RET from this donor to all N acceptors within a given region is

$$k_T = \frac{1}{\tau_D}\left[1 + \sum_{i=1}^{N}\left(\frac{R_0}{R_i}\right)^6\right] \tag{2}$$

where τ_D is the donor lifetime in the absence of acceptor, and R_i is the distance between the donor and the i-th acceptor molecule.

The survival probability for the donor molecule in question, $\rho(t)$, can be obtained by solving the differential

Table II. Best Fit Parameters A_i of Eq. (22) to the Numerical Results Obtained for $\beta_w = 0.25$

	β_1							
	0.20	0.40	0.60	0.80	1.00	1.25	1.50	2.00
				$B = 1.05$				
A_0	0.35312	0.39403	0.47780	0.59760	0.72411	0.84369	0.91268	0.96912
A_1	−0.76073	−0.74881	−0.70922	−0.61684	−0.47989	−0.30706	−0.18376	−0.06822
A_2	0.08617	0.02569	−0.08066	−0.19231	−0.25505	−0.23685	−0.17228	−0.07501
A_3	0.51127	0.47531	0.39109	0.24418	0.08054	−0.04757	−0.07880	−0.05018
A_4	0.20357	0.20886	0.20534	0.16582	0.09653	0.02044	−0.01265	−0.01602
				$B = 1.25$				
A_0	0.35022	0.36354	0.43284	0.55409	0.68875	0.82038	0.89850	0.96379
A_1	−0.76314	−0.75028	−0.71517	−0.64083	−0.51707	−0.34360	−0.21052	−0.07973
A_2	0.08902	0.07914	−0.00722	−0.14018	−0.23606	−0.24624	−0.18939	−0.08632
A_3	0.51569	0.49650	0.42330	0.29183	0.12583	−0.02609	−0.07642	−0.05597
A_4	0.20510	0.19765	0.19169	0.17159	0.11501	0.03496	−0.00739	−0.01723
				$B = 1.50$				
A_0	0.35010	0.35590	0.40419	0.51744	0.65566	0.79711	0.88387	0.95814
A_1	−0.76335	−0.75548	−0.72038	−0.65635	−0.54721	−0.37766	−0.23718	−0.09178
A_2	0.08893	0.08828	0.03841	−0.09243	−0.21229	−0.25073	−0.20438	−0.09776
A_3	0.51579	0.50778	0.44550	0.32593	0.16620	−0.00184	−0.07104	−0.06127
A_4	0.20519	0.20074	0.18457	0.17074	0.12853	0.04963	−8.10E − 04	−0.01808
				$B = 2.00$				
A_0	0.35007	0.35288	0.38304	0.47839	0.61472	0.76567	0.86319	0.94986
A_1	−0.76341	−0.75892	−0.72914	−0.67102	−0.57920	−0.42003	−0.27321	−0.10917
A_2	0.08889	0.08995	0.06826	−4.00E − 02	−0.17675	−0.25006	−0.22135	−0.11355
A_3	0.51580	0.51268	0.46858	0.35976	0.21263	0.03365	−0.05932	−0.06757
A_4	0.20521	0.20308	0.18547	0.16748	0.14040	0.06884	9.96 E − 03	−0.01859
				$B = 3.00$				
A_0	0.35006	0.35175	0.37181	0.44853	0.57688	0.73313	0.84052	0.94034
A_1	−0.76343	−0.76054	−0.73707	−0.68345	−0.60475	−0.45972	−0.31058	−0.12880
A_2	0.08888	0.08997	0.08085	−6.61E − 04	−0.13949	−0.24244	−0.23481	−0.13036
A_3	0.51581	0.51431	0.48427	0.38752	0.25246	0.07195	−0.04208	−0.07284
A_4	0.20521	0.20403	0.18969	0.16653	0.14751	0.08721	0.02303	−0.01820

equation

$$-\frac{d\rho(t)}{dt} = k_T\rho(t) = \frac{1}{\tau_D}\left[1 + \sum_1^N \left(\frac{R_0}{R_i}\right)^6\right]\rho(t) \quad (3)$$

with the initial condition $\rho(0) = 1$, leading to

$$\rho(\lambda) = \exp(-\lambda)\prod_{i=1}^{N}\exp\left[-\lambda\left(\frac{R_0}{R_i}\right)^6\right] \quad (4)$$

where $\lambda = t/\tau_D$ is the reduced time. The average decay (taking into account all statistical arrangements of the N acceptor molecules) for a donor located in the center of a finite disk with radius R_d,$\langle\rho(t)\rangle_N$, is given by:

$$\langle\rho(\lambda)\rangle_N = \exp(-\lambda)\prod_{i=1}^{N}\int_0^{R_d}\exp\left[-\lambda\left(\frac{R_0}{R_i}\right)^6\right]W(R_i)\,dR_i \quad (5)$$

where $W(R_i)dR_i$ is the probability of finding acceptor molecule A_i in the ring of inner radius R_i and outer radius $R_i + dR_i$. The acceptor distribution function is normalized, in the sense that

$$\int_0^{R_d} W(R_i)\,dR_i = 1 \quad (6)$$

Because all acceptors have the same distribution function, $W(R_i)dR_i = W(R_j)dR_j =$ simply $W(R)dR$, all integrals in Eq. (5) are identical, and denoting them by $J(\lambda)$, we can write

$$\langle\rho(t)\rangle_N = \exp\left(-\frac{t}{\tau_D}\right)[J(t)]^N \quad (7)$$

We now consider specifically that donors and acceptors are distributed in parallel planes in the bilayer, see Fig. 2. For uniform distribution in a planar disk, $W(R) = 2R/R_d^2$, and Davenport *et al.* [16] showed

Table III. Best Fit Parameters A_i of Eq. (22) to the Numerical Results Obtained for $\beta_w = 0.50$

	β_1							
	0.20	0.40	0.60	0.80	1.00	1.25	1.50	2.00
				$B = 1.05$				
A_0	0.42575	0.47281	0.55919	0.66873	0.77339	0.86834	0.92394	0.97167
A_1	−0.74046	−0.71260	−0.65046	−0.54504	−0.41439	−0.26518	−0.16181	−0.06269
A_2	−0.02101	−0.07537	−0.16154	−0.23575	−0.25899	−0.21946	−0.15657	−0.06942
A_3	0.45028	0.39706	0.29332	0.15147	0.02148	−0.06441	−0.07813	−0.04713
A_4	0.21485	0.20663	0.18191	0.12953	0.06499	0.00655	−0.01572	−0.01529
				$B = 1.25$				
A_0	0.42125	0.44279	0.51845	0.63065	0.74305	0.84831	0.91151	0.96679
A_1	−0.74455	−0.72235	−0.66884	−0.57691	−0.45264	−0.29883	−0.18593	−0.07328
A_2	−0.01723	−0.03065	−0.10775	−0.20355	−0.25305	−0.23270	−0.17356	−0.08002
A_3	0.45691	0.42674	0.33551	0.19910	0.05865	−0.05001	−0.07842	−0.05281
A_4	0.21731	0.20489	0.18363	0.14403	0.08364	0.01802	−0.01214	−0.01659
				$B = 1.50$				
A_0	0.42082	0.43303	0.49183	0.59897	0.71508	0.82859	0.89883	0.96165
A_1	−0.74523	−0.72956	−0.68108	−0.59981	−0.48455	−0.33023	−0.20981	−0.08430
A_2	−0.01736	−0.02019	−0.07298	−0.17284	−0.24235	−0.24181	−0.18875	−0.09070
A_3	0.45741	0.44046	0.36298	0.23573	0.09329	−0.03283	−0.07620	−0.05806
A_4	0.21764	0.20881	0.18481	0.15244	0.09907	0.03002	−0.00741	−0.01760
				$B = 2.00$				
A_0	0.42064	0.42805	0.47026	0.56511	0.68098	0.80240	0.88122	0.95422
A_1	−0.74555	−0.73482	−0.69370	−0.62223	−0.51961	−0.36934	−0.24181	−0.10003
A_2	−0.01748	−0.01698	−0.04730	−1.38E − 01	−0.22386	−0.24855	−0.20656	−0.10536
A_3	0.45757	0.44810	0.38827	0.27311	0.13492	−0.00672	−0.06953	−0.06444
A_4	0.21776	0.21213	0.18888	0.15932	0.11534	0.04631	5.83E − 04	−0.01842
				$B = 3.00$				
A_0	0.42055	0.42574	0.45721	0.53841	0.64970	0.77577	0.86225	0.94580
A_1	−0.74570	−0.73775	−0.70355	−0.63971	−0.54870	−0.40625	−0.27473	−0.11758
A_2	−0.01755	−0.01629	−0.03406	−0.10979	−0.20277	−0.24995	−0.22181	−0.12088
A_3	0.45763	0.45153	0.40566	0.30274	0.17214	0.02241	−0.05851	−0.07005
A_4	0.21781	0.21391	0.19372	0.16468	0.12799	0.06267	0.01053	−0.01854

that

$$J(\lambda) = \frac{2w^2}{R_d^2}\int_{w/\sqrt{w^2+R_d^2}}^{1} \exp\left[\left(-\frac{t}{\tau_D}\right)\left(\frac{R_0}{w}\right)^6 \alpha^6\right]\alpha^{-3}d\alpha \quad (8)$$

or, equivalently,

$$J(\lambda) = 1 - \frac{2}{N}\beta_w^2\gamma\int_{w/\sqrt{w^2+R_d^2}}^{1} f(\lambda, \beta_w, \alpha)\, d\alpha \quad (9)$$

where

$$f(\lambda, \beta_w, \alpha) = \left[1 - \exp\left(-\lambda\frac{\alpha^6}{\beta_\omega^6}\right)\right]\alpha^{-3} \quad (10)$$

and γ is the number of acceptors inside a disk of radius R_0 (and is related to the surface molecular density n through $\gamma = n\pi R_0^2$), $\alpha = \cos\theta$ in Fig. 2, and $\beta_w = w/R_0$ is the reduced interplanar spacing.

We now assume a step function (with an exclusion region for $R <$ plane R_1, and an acceptor-enriched region

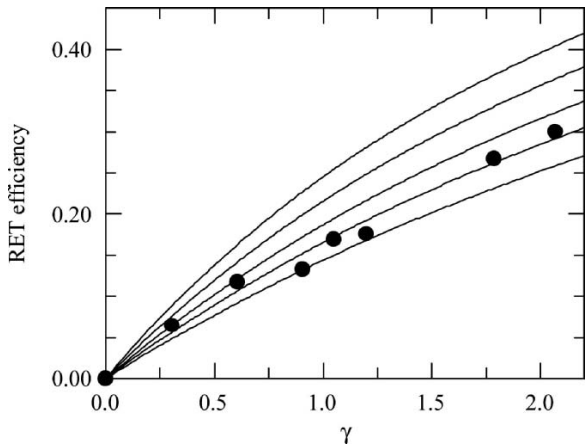

Fig. 4. Approximate theoretical RET efficiency curves for $\beta_w = w/R_0 = 0.375$ and $\beta_1 = R_1/R_0 = 1.25$ (from *bottom to top*: $B = 1.05$, $B = 1.25$, $B = 1.5$, $B = 2$, $B = 3$; see text for approximation details) and experimental results of RET between AcChR tryptophan and *t*-PnA in egg-PC/DMPA/cholesterol (2:1:1) vesicles [15]. The best fit is obtained for $B = 1.25$.

Table IV. Best Fit Parameters A_i of Eq. (22) to the Numerical Results Obtained for $\beta_w = 0.75$

	β_1							
	0.20	0.40	0.60	0.80	1.00	1.25	1.50	2.00
				$B = 1.05$				
A_0	0.56017	0.60628	0.68005	0.76197	0.83415	0.89893	0.93853	0.97527
A_1	−0.65195	−0.60905	−0.53245	−0.43025	−0.32266	−0.20987	−0.13255	−0.05482
A_2	−0.16515	−0.19899	−0.24089	−0.25934	−0.24212	−0.18932	−0.13363	−0.06134
A_3	0.29350	0.23307	0.13676	0.03463	−0.03979	−0.07699	−0.07394	−0.04249
A_4	0.18363	0.16208	0.12310	0.07240	0.02618	−0.00776	−0.01818	−0.01409
				$B = 1.25$				
A_0	0.55477	0.58135	0.64807	0.73268	0.81092	0.88326	0.92844	0.97102
A_1	−0.65750	−0.62798	−0.56181	−0.46607	−0.35817	−0.23844	−0.15283	−0.06410
A_2	−0.16175	−0.17470	−0.21723	−0.25164	−0.24953	−0.20541	−0.14966	−0.07085
A_3	0.30111	0.26476	0.17785	0.07115	−0.01705	−0.07124	−0.07707	−0.04791
A_4	0.18676	0.17067	0.13737	0.09010	0.04088	−6.92E − 04	−0.01659	−0.01548
				$B = 1.50$				
A_0	0.55394	0.57180	0.62754	0.70923	0.79020	0.86824	0.91837	0.96662
A_1	−0.65863	−0.63691	−0.58008	−0.49257	−0.38794	−0.26480	−0.17262	−0.07363
A_2	−0.16167	−0.16749	−0.20135	−0.24217	−0.25236	−0.21816	−0.16420	−0.08036
A_3	0.30221	0.27781	0.20384	0.10050	0.00523	−0.06305	−0.07829	−0.05297
A_4	0.18737	0.17544	0.14598	0.10306	0.05401	0.00704	−1.41E − 02	−0.01663
				$B = 2.00$				
A_0	0.55352	0.56590	0.61010	0.68470	0.76576	0.84892	0.90477	0.96038
A_1	−0.65923	−0.64326	−0.59610	−0.51879	−0.42093	−0.29727	−0.19864	−0.08701
A_2	−0.16169	−0.16420	−0.18842	−2.30E − 01	−0.25183	−0.23105	−0.18166	−0.09327
A_3	0.30273	0.28610	0.22629	0.13113	0.03306	−0.04943	−0.07726	−0.05925
A_4	0.18768	0.17900	0.15378	0.11570	0.06912	0.01795	−9.63E − 03	−0.01778
				$B = 3.00$				
A_0	0.55331	0.56270	0.59857	0.66526	0.74389	0.82990	0.89057	0.95347
A_1	−0.65954	−0.64702	−0.60729	−0.53886	−0.44873	−0.32771	−0.22493	−0.10162
A_2	−0.16172	−0.16291	−0.18059	−2.19E − 01	−0.24835	−0.24028	−0.19738	−0.10680
A_3	0.30298	0.29057	0.24151	0.15546	0.05885	−0.03333	−0.07334	−0.06501
A_4	0.18783	0.18112	0.15949	0.12533	0.08213	0.02934	−0.00376	−0.01846

for $R_1 < R < R_2$) for the local acceptor concentration as a function of distance to each donor, Fig. 1. The acceptor distribution function is given by

$$W(R) = \begin{cases} 0 & \Leftarrow R \le R_1 \\ \frac{2BR}{R_d^2} & \Leftarrow R_1 < R < R_2 \\ \frac{2R}{R_d^2} & \Leftarrow R_2 < R < R_d \end{cases} \tag{11}$$

The B parameter is the factor of acceptor enrichment in the donor immediate vicinity, relative to a uniform distribution, and it is related to R_1 and R_2 through the relationship (which is a consequence of the normalization of $W(R)$):

$$B = \frac{R_2^2}{R_2^2 - R_1^2} \Leftrightarrow R_2 = \sqrt{\frac{B}{B-1}} R_1 \tag{12}$$

For this acceptor distribution, $J(\lambda)$ can be partitioned into three integrals, $J_0(\lambda)$, $J_1(\lambda)$, and $J_2(\lambda)$,

$$J(\lambda) = J_0(\lambda) + J_1(\lambda) + J_2(\lambda) \tag{13}$$

defined over the the regions $R < R_1$, $R_1 < R < R_2$, and $R_2 < R < R_d$, respectively. As there are no acceptors for $R < R_1$, it follows that $J_0(\lambda) = 0$. $J_2(\lambda)$ is very similar to $J(\lambda)$ in the uniform case (Eqs. (8) and (9)), with the difference that the upper limit is not 1 (which would correspond to $\theta = \pi/2$ or $R_2 = 0$), but $w/(w^2 + R_2^2)^{1/2}$. We can write

$$\begin{aligned} J_2(\lambda) &= \frac{2w^2}{R_d^2} \int_{w/\sqrt{w^2+R_d^2}}^{w/\sqrt{w^2+R_2^2}} \exp\left(-\lambda \frac{\alpha^6}{\beta_w^6}\right) \alpha^{-3}\, d\alpha \\ &= \frac{2w^2}{R_d^2} \left(\int_{w/\sqrt{w^2+R_d^2}}^{w/\sqrt{w^2+R_2^2}} \alpha^{-3}\, d\alpha \right. \\ &\quad \left. - \int_{w/\sqrt{w^2+R_d^2}}^{w/\sqrt{w^2+R_2^2}} f(\lambda, \beta_w, \alpha)\, d\alpha \right) \end{aligned} \tag{14}$$

Table V. Best Fit Parameters A_i of Eq. (22) to the Numerical Results Obtained for $\beta_w = 1.00$

	β_1							
	0.20	0.40	0.60	0.80	1.00	1.25	1.50	2.00
				$B = 1.05$				
A_0	0.72125	0.75183	0.79770	0.84595	0.88803	0.92724	0.95295	0.97925
A_1	−0.48424	−0.44410	−0.37924	−0.30333	−0.23000	−0.15527	−0.10273	−0.04604
A_2	−0.25569	−0.25920	−0.25548	−0.23550	−0.20123	−0.15164	−0.10787	−0.05211
A_3	0.08387	0.04655	−0.00508	−0.04932	−0.07375	−0.07753	−0.06553	−0.03690
A_4	0.09864	0.07898	0.04921	0.01910	−0.00313	−0.01644	−0.01856	−0.01252
				$B = 1.25$				
A_0	0.71751	0.73604	0.77685	0.82633	0.87200	0.91589	0.94525	0.97572
A_1	−0.48915	−0.46408	−0.40836	−0.33451	−0.25848	−0.17749	−0.11875	−0.05383
A_2	−0.25523	−0.25606	−0.25651	−0.24434	−0.21566	−0.16776	−0.12196	−0.06031
A_3	0.08852	0.06623	0.01862	−0.03189	−0.06575	−0.07855	−0.07050	−0.04187
A_4	0.10109	0.08891	0.06266	0.03121	0.00489	−1.35E − 02	−0.01859	−0.01392
				$B = 1.50$				
A_0	0.71682	0.73002	0.76450	0.81173	0.85848	0.90545	0.93781	0.97213
A_1	−0.49012	−0.47192	−0.42514	−0.35677	−0.28162	−0.19742	−0.13397	−0.06168
A_2	−0.25526	−0.25527	−0.25626	−0.24891	−0.22568	−0.18104	−0.13468	−0.06839
A_3	0.08933	0.07363	0.03300	−0.01760	−0.05703	−0.07762	−0.07404	−0.04654
A_4	0.10156	0.09278	0.07053	0.04041	0.01230	−0.00998	−1.80E − 02	−0.01513
				$B = 2.00$				
A_0	0.71645	0.72608	0.75422	0.79722	0.84338	0.89265	0.92814	0.96718
A_1	−0.49065	−0.47720	−0.43899	−0.37820	−0.30661	−0.22121	−0.15338	−0.07244
A_2	−0.25530	−0.25498	−0.25582	−2.52E − 01	−0.23481	−0.19547	−0.14998	−0.07918
A_3	0.08975	0.07842	0.04509	−0.00259	−0.04555	−0.07434	−0.07696	−0.05236
A_4	0.10181	0.09536	0.07709	0.04961	0.02108	−0.00479	−1.65E − 02	−0.01649
				$B = 3.00$				
A_0	0.71626	0.72381	0.74734	0.78606	0.83045	0.88062	0.91847	0.96186
A_1	−0.49093	−0.48029	−0.44826	−0.39430	−0.32732	−0.24294	−0.17239	−0.08386
A_2	−0.25533	−0.25491	−0.25551	−2.54E − 01	−0.24108	−0.20729	−0.16395	−0.09027
A_3	0.08997	0.08114	0.05322	0.00939	−0.03452	−0.06941	−0.07815	−0.05785
A_4	0.10193	0.09686	0.08150	0.05671	0.02888	8.14E − 04	−0.01409	−0.01755

After calculation of the first integral in the latter equation, one obtains

$$J_2(\lambda) = 1 - \left(\frac{R_2}{R_d}\right)^2 - \frac{2w^2}{R_d^2}\int_{w/\sqrt{w^2+R_d^2}}^{w/\sqrt{w^2+R_2^2}} f(\lambda, \beta_w, \alpha)\, d\alpha \tag{15}$$

$J_1(\lambda)$ is obtained similarly, replacing R_2 with R_1, R_d with R_2, and multiplying by the acceptor enrichment factor in this region, B:

$$\begin{aligned} J_2(\lambda) &= B\frac{2w^2}{R_d^2}\int_{w/\sqrt{w^2+R_2^2}}^{w/\sqrt{w^2+R_1^2}} \exp\left(-\lambda\frac{\alpha^6}{\beta_w^6}\right)\alpha^{-3}\, d\alpha \\ &= B\frac{2w^2}{R_d^2}\left(\int_{w/\sqrt{w^2+R_2^2}}^{w/\sqrt{w^2+R_1^2}} \alpha^{-3}\, d\alpha \right. \\ &\quad \left. - \int_{w/\sqrt{w^2+R_2^2}}^{w/\sqrt{w^2+R_1^2}} f(\lambda, \beta_w, \alpha)\, d\alpha\right) \end{aligned} \tag{16}$$

and, after integration of the α^{-3} term,

$$\begin{aligned} J_2(\lambda) = {} & \frac{BR_2^2}{R_d^2} - \frac{BR_1^2}{R_d^2} \\ & - \frac{2w^2B}{R_d^2}\int_{w/\sqrt{w^2+R_d^2}}^{w/\sqrt{w^2+R_2^2}} f(\lambda, \beta_w, \alpha)\, d\alpha \end{aligned} \tag{17}$$

Inserting the results of Eqs. (15) and (17) into Eq. (13):

$$\begin{aligned} J(\lambda) = {} & 1 + \frac{1}{R_d^2}[R_2^2(B-1) - BR_1^2] \\ & - \frac{2w^2}{R_d^2}\left[\int_{w/\sqrt{w^2+R_d^2}}^{w/\sqrt{w^2+R_2^2}} f(\lambda, \beta_w, \alpha)\, d\alpha \right. \\ & \left. - B\int_{w/\sqrt{w^2+R_d^2}}^{w/\sqrt{w^2+R_2^2}} f(\lambda, \beta_w, \alpha)\, d\alpha\right] \end{aligned} \tag{18}$$

Table VI. Best Fit Parameters A_i of Eq. (22) to the Numerical Results Obtained for $\beta_w = 1.25$

	β_1							
	0.20	0.40	0.60	0.80	1.00	1.25	1.50	2.00
				$B = 1.05$				
A_0	0.84336	0.85796	0.88062	0.90504	0.92726	0.94939	0.96517	0.98310
A_1	−0.30776	−0.28313	−0.24343	−0.19837	−0.15523	−0.11017	−0.07677	−0.03750
A_2	−0.23740	−0.22756	−0.20859	−0.18204	−0.15161	−0.11452	−0.08345	−0.04292
A_3	−0.04759	−0.05801	−0.07074	−0.07813	−0.07753	−0.06803	−0.05457	−0.03103
A_4	0.02056	0.01218	3.27E − 04	−0.01008	−0.01644	−0.01868	−0.01696	−0.01075
				$B = 1.25$				
A_0	0.84166	0.84996	0.86892	0.89319	0.91697	0.94159	0.95954	0.98026
A_1	−0.31059	−0.29659	−0.26400	−0.22041	−0.17539	−0.12627	−0.08881	−0.04382
A_2	−0.23847	−0.23287	−0.21858	−0.19543	−0.16631	−0.12835	−0.09499	−0.04974
A_3	−0.04632	−0.05225	−0.06437	−0.07511	−0.07857	−0.07243	−0.06006	−0.03541
A_4	0.02155	0.01679	0.00638	−0.00525	−0.01383	−1.84E − 02	−0.01792	−0.01208
				$B = 1.50$				
A_0	0.84135	0.84723	0.86280	0.88524	0.90896	0.93482	0.95433	0.97744
A_1	−0.31112	−0.30118	−0.27459	−0.23490	−0.19078	−0.14002	−0.09982	−0.05003
A_2	−0.23868	−0.23468	−0.22338	−0.20355	−0.17678	−0.13959	−0.10518	−0.05633
A_3	−0.04610	−0.05027	−0.06063	−0.07213	−0.07818	−0.07519	−0.06440	−0.03949
A_4	0.02173	0.01836	0.00968	−0.00164	−0.01127	−0.01764	−1.84E − 02	−0.01326
				$B = 2.00$				
A_0	0.84119	0.84548	0.85800	0.87788	0.90061	0.92700	0.94789	0.97369
A_1	−0.31140	−0.30414	−0.28284	−0.24809	−0.20655	−0.15567	−0.11327	−0.05828
A_2	−0.23880	−0.23586	−0.22698	−2.10E − 01	−0.18686	−0.15176	−0.11718	−0.06491
A_3	−0.04598	−0.04901	−0.05754	−0.06879	−0.07679	−0.07727	−0.06887	−0.04455
A_4	0.02183	0.01937	0.01232	0.00191	−0.00818	−0.01624	−1.86E − 02	−0.01463
				$B = 3.00$				
A_0	0.84110	0.84448	0.85489	0.87250	0.89386	0.92004	0.94176	0.96980
A_1	−0.31155	−0.30583	−0.28815	−0.25761	−0.21908	−0.16936	−0.12590	−0.06674
A_2	−0.23886	−0.23654	−0.22924	−2.15E − 01	−0.19443	−0.16186	−0.12798	−0.07351
A_3	−0.04592	−0.04830	−0.05548	−0.06604	−0.07500	−0.07818	−0.07224	−0.04935
A_4	0.02187	0.01995	0.01405	0.00463	−0.00541	−1.46E − 02	−0.01836	−0.01582

Taking into account the interdependence of R_1, R_2, and B (Eq. (12)), the second term on the latter equation vanishes. Using $\gamma = n\pi R_0^2$ and $N = n\pi R_d^2$, one obtains

$$J(\lambda) = 1 - \frac{2}{N}\beta_w^2\gamma\left[\int_{w/\sqrt{w^2+R_d^2}}^{w/\sqrt{w^2+R_2^2}} f(\lambda, \beta_w, \alpha)\, d\alpha - B\int_{w/\sqrt{w^2+R_2^2}}^{w/\sqrt{w^2+R_1^2}} f(\lambda, \beta_w, \alpha)\, d\alpha\right] \tag{19}$$

Inserting this expression for $J(t)$ in Eq. (7), and taking the limit ($N\to\infty$, $R_d\to\infty$), one obtains the macroscopic decay law. The result is

$$i(\lambda) = \exp\left(-\lambda - 2\beta_w^2\gamma\left[\int_0^{\beta_w/\sqrt{\beta_w^2+\beta_2^2}} f(\lambda, \beta_w, \alpha)\, d\alpha - B\int_{\beta_w/\sqrt{\beta_w^2+\beta_2^2}}^{\beta_w/\sqrt{\beta_w^2+\beta_1^2}} f(\lambda, \beta_w, \alpha)\, d\alpha\right]\right) \tag{20}$$

In this equation, $\beta_1 = R_1/R_0$ and $\beta_2 = R_2/R_0$ were introduced, to show that i is in fact a function of five dimensionless variables: a dimensionless average concentration γ, the reduced time λ, the reduced interplanar spacing β_w, the reduced exclusion distance β_1, and the relative enrichment factor for the acceptor in the annular region, B. As noted above, β_2 is not an independent parameter, as it is determined by the values of β_1 and B.

The integrals in Eq. (20) present a minor problem (as pointed out in Ref. [16]), because f is not defined for $\alpha = 0$ or $\beta_w = 0$ (see Eq. (9)). One way to deal with the singularity for $\alpha\to 0$ would be to expand f in an infinite series of powers of α, and carry out integration of each term of the series, thus obtaining an analytical expression for the decay law. Another possibility is to note that $\lim_{\alpha\to 0} f(\lambda, \beta_w, 0) = 0$ for $\beta_w \neq 0$, and carry out the numerical integration. We found that the latter option is much more convenient from the numerical point of view. There is still the problem for $\beta_w = 0$ (planar geometry). To cir-

Table VII. Best Fit Parameters A_i of Eq. (22) to the Numerical Results Obtained for $\beta_w = 1.50$

	β_1							
	0.20	0.40	0.60	0.80	1.00	1.25	1.50	2.00
				$B = 1.05$				
A_0	0.91333	0.91947	0.92981	0.94159	0.95298	0.96518	0.97461	0.98649
A_1	−0.18253	−0.17059	−0.15015	−0.12628	−0.10267	−0.07675	−0.05626	−0.02991
A_2	−0.17149	−0.16302	−0.14770	−0.12841	−0.10781	−0.08344	−0.06283	−0.03457
A_3	−0.07891	−0.07868	−0.07693	−0.07253	−0.06550	−0.05456	−0.04336	−0.02545
A_4	−0.01289	−0.01463	−1.69E − 02	−0.01844	−0.01856	−0.01696	−0.01432	−0.00897
				$B = 1.25$				
A_0	0.91268	0.91583	0.92372	0.93481	0.94663	0.95997	0.97061	0.98426
A_1	−0.18379	−0.17768	−0.16222	−0.14007	−0.11590	−0.08788	−0.06501	−0.03491
A_2	−0.17237	−0.16807	−0.15683	−0.13970	−0.11951	−0.09412	−0.07177	−0.04008
A_3	−0.07891	−0.07884	−0.07810	−0.07531	−0.06972	−0.05966	−0.04841	−0.02916
A_4	−0.01270	−0.01361	−0.01564	−0.01769	−0.01864	−1.79E − 02	−0.01560	−0.01016
				$B = 1.50$				
A_0	0.91257	0.91474	0.92096	0.93077	0.94213	0.95577	0.96709	0.98212
A_1	−0.18401	−0.17979	−0.16765	−0.14820	−0.12516	−0.09680	−0.07262	−0.03967
A_2	−0.17252	−0.16956	−0.16083	−0.14612	−0.12741	−0.10242	−0.07936	−0.04527
A_3	−0.07891	−0.07887	−0.07844	−0.07655	−0.07216	−0.06328	−0.05246	−0.03256
A_4	−0.01267	−0.01330	−0.01497	−0.01705	−0.01843	−0.01833	−1.65E − 02	−0.01122
				$B = 2.00$				
A_0	0.91251	0.91407	0.91894	0.92731	0.93779	0.95121	0.96298	0.97938
A_1	−0.18412	−0.18109	−0.17162	−0.15510	−0.13403	−0.10636	−0.08146	−0.04576
A_2	−0.17260	−0.17047	−0.16371	−1.51E − 01	−0.13477	−0.11108	−0.08798	−0.05181
A_3	−0.07891	−0.07888	−0.07863	−0.07739	−0.07412	−0.06670	−0.05677	−0.03671
A_4	−0.01265	−0.01311	−0.01445	−0.01639	−0.01804	−0.01859	−1.74E − 02	−0.01246
				$B = 3.00$				
A_0	0.91248	0.91370	0.91768	0.92492	0.93448	0.94740	0.95928	0.97665
A_1	−0.18418	−0.18181	−0.17407	−0.15984	−0.14073	−0.11429	−0.08936	−0.05178
A_2	−0.17264	−0.17098	−0.16548	−1.55E − 01	−0.14019	−0.11808	−0.09549	−0.05816
A_3	−0.07891	−0.07889	−0.07872	−0.07785	−0.07536	−0.06920	−0.06026	−0.04059
A_4	−0.01264	−0.01300	−0.01411	−0.01589	−0.01762	−1.86E − 02	−0.01794	−0.01356

cumvent this, we calculated the decays for very small values of this parameter, and verified that the results converged for $\beta_w < 0.01$. In case of $B = 1$, it was possible to verify the result of Wolber and Hudson [13] for uniform acceptor distribution. All results shown for $\beta_w = 0$ in the next section were calculated this way.

After the decay law is computed, the RET efficiency is calculated again by numerical integration:

$$E = 1 - \int_0^\infty i(\lambda)\, d\lambda \tag{21}$$

RESULTS AND DISCUSSION

Numerical Results and Empirical Fits

Our methodology consisted in calculating the RET efficiencies (from integration of the decays, Eq. (21)) for chosen values of $B \in [1.05, 3]$, $\beta_w \in [0.25, 2]$ and $\beta_1 \in [0.2, 2]$. For each (B, β_w, β_1) triad, E was calculated for 30 equally spaced γ values in the [0, 3] range, and these (γ, E) pairs were fitted to empirical functions of the form

$$1 - E = A_0 + A_1[\log_{10}(\gamma)] + A_2[\log_{10}(\gamma)]^2 + A_3[\log_{10}(\gamma)]^3 + A_4[\log_{10}(\gamma)]^4 \tag{22}$$

These 4th-degree polynomials in $\log_{10}(\gamma)$ fitted very well to the data for all (B, β_w, β_1) combinations. As an example, Fig. 3 shows the computed $1-E$ values and the fitting curves for $\beta_w = 0$ (planar system) and $\beta_1 = 1.5$. The maximum relative deviation between the numerical results and the fitted curves for the 150 points shown was 1.9%, and the average deviation was 0.2%. Tables I–VIII show all A_i coefficients recovered from all (γ, E) fits for all explored (B, β_w, β_1) triads. Each table refers to a fixed β_w value (0, 0.25, 0.5, 0.75, 1.0, 1.25, 1.5, and 2.0) and

Table VIII. Best Fit Parameters A_i of Eq. (22) to the Numerical Results Obtained for $\beta_w = 2.00$

	β_1							
	0.20	0.40	0.60	0.80	1.00	1.25	1.50	2.00
				$B = 1.05$				
A_0	0.96979	0.97092	0.97319	0.97613	0.97929	0.98311	0.98650	0.99158
A_1	−0.06678	−0.06432	−0.05936	−0.05293	−0.04596	−0.03747	−0.02990	−0.01845
A_2	−0.07356	−0.07108	−0.06603	−0.05937	−0.05203	−0.04288	−0.03456	−0.02163
A_3	−0.04940	−0.04805	−0.04521	−0.04132	−0.03685	−0.03101	−0.02544	−0.01636
A_4	−0.01584	−0.01551	−1.48E − 02	−0.01377	−0.01250	−0.01074	−0.00897	−0.00591
				$B = 1.25$				
A_0	0.96969	0.97017	0.97158	0.97395	0.97692	0.98086	0.98454	0.99026
A_1	−0.06699	−0.06597	−0.06289	−0.05772	−0.05120	−0.04249	−0.03430	−0.02143
A_2	−0.07378	−0.07274	−0.06963	−0.06434	−0.05756	−0.04831	−0.03941	−0.02503
A_3	−0.04952	−0.04896	−0.04724	−0.04423	−0.04023	−0.03451	−0.02871	−0.01880
A_4	−0.01587	−0.01573	−0.01532	−0.01455	−0.01347	−1.18E − 02	−0.01002	−0.00675
				$B = 1.50$				
A_0	0.96968	0.96999	0.97102	0.97293	0.97556	0.97931	0.98302	0.98910
A_1	−0.06703	−0.06635	−0.06411	−0.05994	−0.05419	−0.04592	−0.03768	−0.02405
A_2	−0.07381	−0.07313	−0.07087	−0.06662	−0.06068	−0.05198	−0.04310	−0.02800
A_3	−0.04954	−0.04917	−0.04793	−0.04554	−0.04210	−0.03681	−0.03115	−0.02090
A_4	−0.01587	−0.01578	−0.01548	−0.01489	−0.01398	−0.01249	−1.08E − 02	−0.00747
				$B = 2.00$				
A_0	0.96967	0.96989	0.97065	0.97218	0.97442	0.97784	0.98145	0.98773
A_1	−0.06704	−0.06657	−0.06491	−0.06159	−0.05669	−0.04915	−0.04118	−0.02714
A_2	−0.07383	−0.07335	−0.07167	−6.83E − 02	−0.06327	−0.05541	−0.04690	−0.03147
A_3	−0.04955	−0.04929	−0.04837	−0.04649	−0.04362	−0.03893	−0.03360	−0.02332
A_4	−0.01587	−0.01581	−0.01559	−0.01513	−0.01439	−0.01310	−1.15E − 02	−0.00827
				$B = 3.00$				
A_0	0.96966	0.96983	0.97044	0.97170	0.97364	0.97675	0.98017	0.98648
A_1	−0.06705	−0.06669	−0.06537	−0.06262	−0.05839	−0.05157	−0.04400	−0.02993
A_2	−0.07384	−0.07347	−0.07214	−6.94E − 02	−0.06503	−0.05795	−0.04993	−0.03459
A_3	−0.04955	−0.04935	−0.04863	−0.04708	−0.04463	−0.04046	−0.03553	−0.02546
A_4	−0.01587	−0.01583	−0.01565	−0.01528	−0.01465	−1.35E − 02	−0.01211	−0.00898

varying B (1.05, 1.25, 1.5, 2, and 3) and β_1 (0.2, 0.4, 0.6, 0.8, 1.0, 1.25, 1.5, and 2.0) values.

Example of Application to Analysis of Experimental RET Data

In a typical experiment, RET efficiencies are measured for several values of acceptor concentration, and R_0 is calculated from spectroscopic data concerning the donor and acceptor probes (as described, e.g., in Ref. [4]). Three unknowns remain at this stage, namely, R_1, w, and B (or, equivalently, β_1, β_w, and B). Due to correlation between these parameters, it is not feasible to recover them all from a single RET experiment. Thus, R_1 and w should be fixed to values obtained from other structural studies (e.g., X-ray diffraction or electron microscopy; for R_1 see for example [17, 18]). Should either R_1 or w be unknown, a possibility is to measure RET to an acceptor probe which displays no preferential affinity for any lipid phase and which should distribute uniformly even for nonuniform lipid distribution (e.g., 1,6-diphenylhexatriene [15]), and obtain the unknown parameter by comparing the curves with $B = 1$ with the experimental data. However, B is usually the parameter of interest, which cannot be obtained from other methodologies, apart from electron spin spectroscopy (see e.g., Ref. [19] for a review) and is the sole optimized parameter in the RET analysis.

As an illustration of the utility of the presented formalism and numerical results, RET data from the tryptophan (Trp) residues of the nicotinic acetylcholine receptor (AcChR) from *Torpedo marmorata* to *trans*-parinaric acid (*t*-PnA) in egg phosphatidylcholine (egg-PC)/1,2-dimirystoyl-*sn*-glycero-phosphatidic acid (DMPA)/cholesterol (2:1:1) vesicles (for which there is no evidence of phase separation in the absence of protein), obtained by Poveda *et al*. [15], are analyzed. These authors calculated $R_0 = 26.8$ Å for the AcChR Trp/*t*-PnA pair, and propose $w = 10$ and $R_1 \cong 35$ Å, which results in $\beta_w = 1.306$

and $\beta_1 = 0.373$. One could use these values and obtain numerically (γ, E) curves for different B values, and verify which B value led to the best fit to the experimental data. Instead, we used an approximate procedure, to illustrate a more probable approximate (and rapid) use of our results by experimental researchers. Whereas no numerical results were obtained specifically for $\beta_w = 1.306$, polynomial coefficients are given in this report for $\beta_w = 1.25$. On the other hand, $\beta_1 = 0.373$ falls almost midway between $\beta_1 = 0.25$ and $\beta_1 = 0.50$, the closest values for which there are polynomial coefficients in the tables. One would expect then a researcher to interpolate the polynomial coefficients given here for (β_w, β_1) = (1.25, 0.25) and (β_w, β_1) = (1.25, 0.50), and plot the curves for all B values available, together with the experimental data (Fig. 4). Visually, it is clear that the best overall B value for the whole (γ, E) range is $B = 1.25$. More quantitatively, one can sum the square of the difference between the experimental and approximate theoretical E values. This sum is equal in this case to 9.9×10^{-4} for $B = 1.25$, compared to 4.1×10^{-3} for $B = 1.05$ and 5.4×10^{-3} for $B = 1.5$.

t-PnA is a fluorescent probe notable for its preferential partition to the ordered gel phase, rather than the disordered liquid crystalline phase, in phase-separated bilayers [20]. Of the two phospholipids in the mixed system, DMPA is in the gel phase at room temperature, whereas egg-PC is in the fluid phase. Therefore, if the presence of AcChR induces heterogeneity of phospholipid distribution, *t*-PnA will be expected to be preferably located in the more ordered, DMPA-enriched domains. Thus, the recovery of $B = 1.25$ for *t*-PnA indicates a moderate enrichment of this probe in the vicinity of AcChR, compatible with preferential location of DMPA around the protein. This is a specific effect for phosphatidic acid, which is not observed for other phospholipid classes (phosphatidylcholine, phosphatidylserine, and phosphatidylglycerol). On the other hand, in the absence of protein, all the phospholipid classes, including phosphatidic acid, exhibit ideal mixing behavior. Since phosphatidic acid and cholesterol have been implicated in functional modulation of the reconstituted AcChR, it is suggested that such a specific modulatory role could be mediated by domain segregation of the relevant lipid classes, and may be important for the protein function [15].

CONCLUSIONS

In this report, a formalism for RET in bilayer systems with heterogeneity in acceptor distribution around each cylindrical donor is presented. There are three regions: an exclusion region closest to the donor ($R < R_1$), a region for which the acceptor concentration is equal to the overall value ($R > R_2$), and, in between, the annular region ($R_1 < R < R_2$), for which there is an increased probability of finding acceptors. The resulting local acceptor concentration is a step-function of the donor–acceptor distance.

The analytical law for the donor decay in the presence of acceptor is given as a function of five dimensionless variables: a dimensionless average concentration γ, the reduced time λ, the reduced interplanar spacing β_w, the reduced exclusion distance β_1, and the relative enrichment factor for the acceptor in the annular region, B. Numerical integration of the decay equation over time was carried out, in order to calculate numerical RET efficiency curves (γ, E) for chosen (B, β_w, β_1) triads. Empirical functions described by five parameters could fit well to the numerical results, and values of the parameters are given for all (B, β_w, β_1) sets. Finally, an application of the formalism to experimental RET data is presented, illustrating how biophysically meaningful information (such as protein-induced heterogeneity of lateral lipid distribution) can be straightforwardly obtained with this method.

ACKNOWLEDGMENT

L. M. S. L. acknowledges financial support from POCTI projects (FCT).

REFERENCES

1. T. Förster (1949). Experimentelle und theoretische Untersuchung des zwischenmolekularen Ubergangs von Elektronennanregungsenergie. *Z. Naturforsch. A* **4**, 321–327.
2. S. R. Rotman and F. X. Hartmman (1988). Non-radiative energy transfer in non-uniform codoped laser crystals. *Chem. Phys. Lett.* **152**, 311–318.
3. J. P. S. Farinha, J. M. G. Martinho, A. Yekta, and M. A. Winnik (1995). Direct nonradiative energy-transfer in polymer interphases—fluorescence decay functions from concentration profiles generated by Fickian diffusion. *Macromolecules* **28**, 6084–6088.
4. L. M. S. Loura, R. F. M. de Almeida, and M. Prieto (2001). Detection and characterization of membrane microheterogeneity by resonance energy transfer. *J. Fluoresc.* **11**, 197–209.
5. L. M. S. Loura, A. Fedorov, and M. Prieto (2001). Fluid–fluid membrane microheterogeneity: A fluorescence resonance energy transfer study. *Biophys. J.* **80**, 776–788.
6. R. F. M. de Almeida, L. M. S. Loura, A. Fedorov, and M. Prieto (2005). Lipid rafts have different sizes depending on membrane composition: A time-resolved fluorescence resonance energy transfer study. *J. Mol. Biol.* **346**, 1109–1120.
7. C. Gutierrez-Merino (1981). Quantitation of the Förster energy transfer for two-dimensional systems. I. Lateral phase separation in unilamellar vesicles formed by binary phospholipids mixtures. *Biophys. Chem.* **14**, 247–257.

8. C. Gutierrez-Merino (1981). Quantitation of the Förster energy transfer for two-dimensional systems. II. Protein distribution and aggregation state in biological membranes. *Biophys. Chem.* **14**, 259–266.
9. C. Gutierrez-Merino, F. Munkonge, A. M. Mata, J. M. East, B. L. Levinson, *et al.* (1987). The position of the ATP binding site on the $(Ca^{2+} + Mg^{2+})$-ATPase. *Biochim. Biophys. Acta* **897**, 207–216.
10. S. S. Antollini, M. A. Soto, I. B. de Romanelli, C. Gutiérrez-Merino, P. Sotomayor, *et al.* (1996). Physical state of bulk and protein-associated lipid in nicotinic acetylcholine receptor-rich membrane studied by laurdan generalized polarization and fluorescence energy transfer. *Biophys. J.* **70**, 1275–1284.
11. I. C. Bonini, S. S. Antollini, C. Gutiérrez-Merino, and F. J. Barrantes (2002). Sphingomyelin composition and physical asymmetries in native acetylcholine receptor-rich membranes. *Eur. Biophys. J.* **31**, 417–427.
12. F. Fernandes, L. M. S. Loura, R. Koehorst, R. B. Spruijt, M. A. Hemminga, *et al.* (2004). Quantification of protein–lipid selectivity using FRET: Application to the M13 major coat protein. *Biophys. J.* **87**, 344–352.
13. P. K. Wolber and B. S. Hudson (1979). An analytical solution to the Förster energy transfer problem in two dimensions. *Biophys. J.* **28**, 197–210.
14. B. Snyder and E. Freire (1982). Fluorescence energy transfer in two dimensions. A numeric solution for random and non-random distributions. *Biophys. J.* 40, 137–148.
15. J. A. Poveda, J. A. Encinar, A. M. Fernández, C. R. Mateo, J. A. Ferragut, *et al.* (2002). Segregation of phosphatidic acid-rich domains in reconstituted acetylcholine receptor membranes. *Biochemistry* **41**, 12253–12262.
16. L. Davenport, R. E. Dale, R. H. Bisby, and R. B. Cundall (1985). Transverse location of the fluorescent probe 1,6-diphenyl-1,3,5-hexatriene in model lipid bilayer membrane systems by resonance excitation energy transfer. *Biochemistry* **24**, 4097–4108.
17. Q. X. Jiang, D. N. Wang, and R. MacKinnon (2004). Electron microscopic analysis of KvAP voltage-dependent K^+ channels in an open conformation. *Nature* **430**, 806–810.
18. Y. Jiang, A. Lee, J. Chen, V. Ruta, M. Cadene, B. T. Chait, *et al.* (2003). X-ray structure of a voltage-dependent K^+ channel. *Nature* **423**, 33–41.
19. D. Marsh and L. I. Horváth (1998). Structure, dynamics and composition of the lipid–protein interface. Perspectives from spin-labelling. *Biochim. Biophys. Acta* **1376**, 267–296.
20. L. A. Sklar, B. S. Hudson, and R. D. Simoni (1977). Conjugated polyene fatty acids as fluorescent probes: Synthetic phospholipid membrane studies. *Biochemistry* **16**, 819–828.